

Spatial Coding Techniques for Molecular MIMO

Martin Damrath*, H. Birkan Yilmaz†, Chan-Byoung Chae†, and Peter Adam Hoehner*

*Faculty of Engineering, Kiel University, Germany, Email: {md, ph}@tf.uni-kiel.de

†School of Integrated Technology, Yonsei University, Korea, Email: {birkan.yilmaz, cbchae}@yonsei.ac.kr

Abstract—This paper studies spatial diversity techniques applied to multiple-input multiple-output (MIMO) diffusion-based molecular communications (DBMC). Two types of spatial coding techniques, namely Alamouti-type coding and repetition MIMO coding are suggested and analyzed. In addition, we consider receiver-side equal-gain combining, which is equivalent to maximum-ratio combining in symmetrical scenarios. For numerical analysis, the channel impulse responses of a symmetrical 2×2 MIMO-DBMC system are acquired by a trained artificial neural network. It is demonstrated that spatial diversity has the potential to improve the system performance and that repetition MIMO coding outperforms Alamouti-type coding.

I. INTRODUCTION

Molecular communication (MC) is a biologically inspired communication paradigm, where molecules are the information carriers [1]. MC is claimed to be a key technology in realizing autonomous nanomachines (NMs), which size ranges from several nanometers up to a few micrometers [2]. The capability of NMs can be enhanced by working in a cooperative manner [3], [4]. Therefore, communication at small scales is at a crucial point. The main application is anticipated to be in the medical sector, where NMs can be used for applications like targeted drug delivery, tissue engineering, or health monitoring [4].

In diffusion-based molecular communication (DBMC) [5], messenger molecules propagate, according to the law of diffusion, from a source to the sink. While this propagation is energy efficient, this communication channel is fundamentally different from the classical radio-based wireless communication channel. For DBMC, the channel impulse response is slowly decreasing, which causes intersymbol interference (ISI) and unreliable transmission [6]. In order to improve this unreliable transmission, spatial diversity can be exploited in multiple-input multiple-output (MIMO) scenarios with multiple antennas at the transmitter and/or receiver side.

MIMO is a familiar topic in classical wireless communication. In molecular communication, however, it has rarely been considered. The authors in [7] were the first to study molecular communication in conjunction with MIMO. They proposed different techniques for transmitter diversity, diversity combining at the receiver side, and spatial multiplexing. Their focus, however, was on multi-user interference, thus neglecting ISI throughout the work. In [8], the authors modeled a MIMO channel taking into account ISI and interlink interference (ILI). They focused then on spatial multiplexing and proposed different detection algorithms. The authors applied their algorithms to a tabletop molecular MIMO testbed and demonstrated an

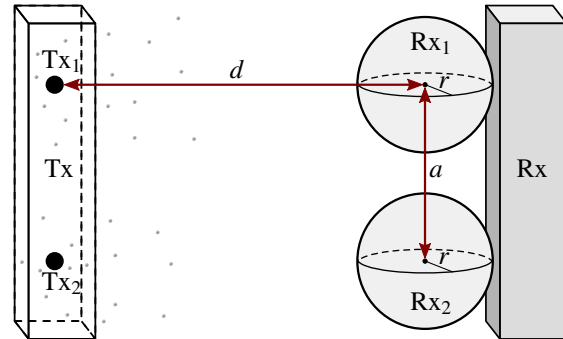


Fig. 1. Model of the diffusion-based molecular 2×2 MIMO system [8].

improvement in the data rate compared to their single-input single-output (SISO) case. In [9], the authors analyzed the influence of a second absorbing receiver on bit error ratio (BER) and capacity for a broadcast MC system.

In this work, the focus is on a MIMO channel considering ISI and ILI. The main contribution is the analysis of different spatial diversity algorithms at the transmitter side. For the transmitter side, we propose Alamouti-type coding and repetition MIMO coding; for the receiver side, we propose equal-gain combining that is equivalent to maximum-ratio combining in symmetrical scenarios. The diversity gain compared to a SISO scenario is investigated by means of a BER simulation, where the influence of the system parameters is shown. The MIMO channel impulse responses are acquired by a trained artificial neural network (ANN).

II. SYSTEM MODEL

A. Topology and Propagation Model

The system model under investigation is similar to the system model introduced in [8] and [10]. As shown in Fig. 1, it consists of a transmitter Tx and a receiver Rx in an infinite three-dimensional homogeneous fluid medium without drift. In the sense of a 2×2 MIMO system, the Tx includes two point antennas Tx_1 and Tx_2 , while the Rx includes two spherical receive antennas Rx_1 and Rx_2 with radius r that are attached to the reflecting body of the Rx. Throughout this work, a symmetrical scenario is assumed where Tx_1 is aligned to Rx_1 and Tx_2 is aligned to Rx_2 . As a result, the distance between Tx_1 and Rx_1 , as well as between Tx_2 and Rx_2 , is given as d . Furthermore, the separation distance between Tx_1 and Tx_2 , as well as between Rx_1 and Rx_2 , is given as a . The fluid medium is described by the diffusion coefficient D .

The molecules emitted by Tx_1 and Tx_2 propagate by Brownian motion, which is described by the Wiener process [11]. Whenever a diffusing molecule hits Rx_1 or Rx_2 , it will be counted and perfectly absorbed, i.e., it will be removed from the environment. As a result, the time histogram of absorbed molecules at Rx_1 and Rx_2 follow the first passage time concept. For a SISO scenario in a 3-dimensional (3-D) environment, there exists a closed-form formula which describes the probability that a molecule hits Rx until time t after its release [12]:

$$F(t) = \frac{r}{d} \operatorname{erfc} \left(\frac{d-r}{\sqrt{4Dt}} \right), \quad (1)$$

where $\operatorname{erfc}(\cdot)$ is the complementary error function. However, for multiple absorbing spheres inside the medium, no such closed-form expression exists. Thus, a corresponding expression to (1) for a given MIMO scenario has to be obtained by either random-walk-based simulations or by using a trained ANN as presented in Section III.

B. Communication Channel

The modulation scheme under investigation is on-off keying (OOK) [13]–[15]. Tx_i emits either no molecules or N messenger molecules at the beginning of a symbol period of length T_s to represent bit $u_i[k] = 0$ or $u_i[k] = 1$, respectively. Molecules emitted by Tx_1 and Tx_2 are of the same type. Furthermore, Rx is assumed to be synchronized with Tx in time domain as suggested in [16]. In addition, Rx_1 and Rx_2 perform strength/energy detection at each symbol duration [17], [18].

The MIMO channel can be separated into subchannels from each transmit antenna Tx_i to each receive antenna Rx_j . Each subchannel is thereby characterized by the corresponding channel coefficients $h_{ji}[\ell]$ ($0 \leq \ell \leq L$), which describe the probability that a molecule hits Rx_j during the ℓ th time slot after its emission at Tx_i . All subchannels can be represented by an equivalent discrete-time channel model with effective channel memory length L [19], [20]. As a result, the number of received molecules at Rx_j can be described by the summation over all subchannels related to Rx_j as

$$y_j[k] = \sum_{i=1}^{N_{\text{Tx}}} \sum_{\ell=0}^L h_{ji}[\ell] x_i[k-\ell] + n_j[k], \quad (2)$$

where N_{Tx} is the number of transmitters, $n_j[k]$ describes the amplitude dependent noise caused by the diffusive propagation of the molecules, and $x_i[k]$ is the discrete-time representation of the modulated data symbol transmitted by Tx_i at the start of the k th transmission interval. For OOK it is defined as

$$x_i[k] = \begin{cases} N & \text{if } u_i[k] = 1 \\ 0 & \text{if } u_i[k] = 0. \end{cases} \quad (3)$$

Since the hitting process of molecules during a bit period can be described by a binomial distribution [21], $y_j[k]$ is represented by the sum over binomial distributions

$$y_j[k] \sim \sum_{i=1}^{N_{\text{Tx}}} \sum_{\ell=0}^L \mathcal{B}(x_i[k-\ell], h_{ji}[\ell]), \quad (4)$$

where $\mathcal{B}(M, p)$ describe a binomial distribution with M number of trials and success probability p .

With the help of (1), the channel coefficients for a SISO scenario can be easily calculated by

$$h[\ell] = F((\ell+1)T_s) - F(\ell T_s). \quad (5)$$

However, for multiple absorbing spheres inside the medium, the channel coefficients $h_{ji}[\ell]$ for a given MIMO scenario has to be obtained by either random-walk-based simulations or by using a trained ANN as presented in Sec. III.

III. ANN FOR CHANNEL MODELING

For modeling a molecular MIMO channel, we utilized the trained ANN of our previous work [22]. A trained ANN is able to estimate the channel coefficients $h_{ji}[\ell]$ for a given MIMO scenario without running simulations.

In a first step, we defined an expected analytical channel response function by introducing fitting parameters into (1). The analytical channel response function at Rx_1 is defined as follows:

$$F_{11}(t, b_1, b_2, b_3) = b_1 \frac{r}{d} \operatorname{erfc} \left(\frac{d-r}{(4D)^{b_2} t^{b_3}} \right), \quad (6)$$

where b_1 , b_2 , and b_3 represent the model fitting parameters. Similarly we define the response at Rx_2 (due to the cross link interference) as follows:

$$F_{21}(t, b_4, b_5, b_6) = b_4 \frac{r}{\sqrt{d^2+a^2}} \operatorname{erfc} \left(\frac{\sqrt{d^2+a^2}-r}{(4D)^{b_5} t^{b_6}} \right), \quad (7)$$

where b_4 , b_5 , and b_6 are also model fitting parameters.

In a second step, we fitted the expected analytical channel response functions to data obtained in extensive simulations. To determine the b_i values, we use a nonlinear least squares curve-fitting technique. These values, in conjunction with selected reference system parameters d , a , r , and D , are the basis of training and test datasets. Hence, the output of the curve-fitting process consists of the model parameters b_i for each selected simulation scenario.

In a third step, after forming the training and test datasets, the training data is fed to the ANN training process. Note that the trained ANN does not require any simulation data. That is, the required inputs are arbitrary system parameters d , a , r , and D . After training, the ANN is able to predict the fitting parameters b_i for these arbitrary system parameters.

In Fig. 2, we present the channel coefficients that are acquired from extensive simulations and the trained ANN. We plot the $h_{11}[k]$ and $h_{21}[k]$ values by utilizing F_{11} , F_{21} , and the symbol duration. Our results validate and support the using of ANN to obtain the channel coefficients.

IV. SPATIAL DIVERSITY

Usually, spatial coding is performed along multiple transmit antennas, whereas combining strategies are applied to multiple receive antennas. In order to achieve a spatial diversity gain at the Tx side, the same information is transmitted over multiple antennas. Therefore, before spatial coding over multiple Tx

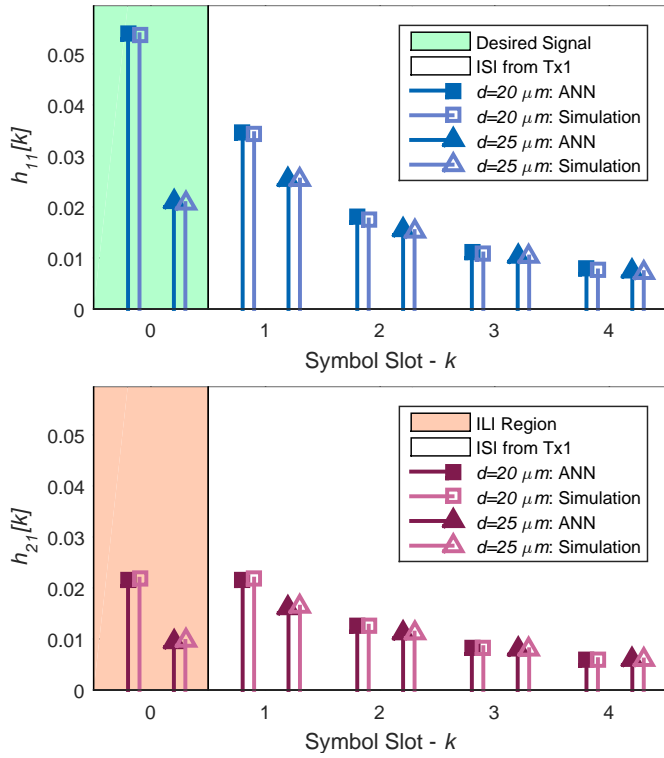


Fig. 2. Comparison of channel coefficients from ANN and simulation data for different distances ($a=13 \mu\text{m}$, $r=5 \mu\text{m}$, $D=200 \mu\text{m}^2/\text{s}$, $T_s=0.4 \text{ s}$)

antennas is applied, the binary data sequence \mathbf{u} is mapped onto a sequence of data symbols \mathbf{s} . Thereby, s_k denotes the k th data symbol of \mathbf{s} . In what follows, two spatial coding techniques are presented - Alamouti-type coding and repetition MIMO coding, respectively. In addition, equal-gain combining, which is equivalent to maximum-ratio combining (MRC) for symmetrical scenarios, is suggested as combining strategy.

A. Alamouti-type Coding

The Alamouti scheme [23] is a space-time block code widely used in radio-based communication systems for spatial diversity. In its origin, the Alamouti code can be represented by the 2×2 transmission matrix

$$\mathbf{G} = \begin{bmatrix} s_k & s_{k+1} \\ -s_{k+1}^* & s_k^* \end{bmatrix}, \quad (8)$$

where the columns of the matrix correspond to the transmit antennas and the rows corresponds to two consecutive transmission intervals $[kT_s, (k+1)T_s]$ and $[(k+1)T_s, (k+2)T_s]$, respectively. As a result, in the first time slot, $x_1[k] = s_k$ is transmitted via the first transmit antenna and $x_2[k] = s_{k+1}$ is transmitted simultaneously via the second transmit antenna. In the second time slot, $x_1[k+1] = -s_{k+1}^*$ is transmitted via Tx_1 and $x_2[k+1] = s_k^*$ is transmitted simultaneously via Tx_2 .

Due to the fact that both transmit antennas emit the same information, a spatial diversity gain can be achieved. The main advantage of the Alamouti scheme is that it is an orthogonal space-time block code, i.e. $\mathbf{G}^H \mathbf{G} = 2\mathbf{I}$, where \mathbf{G}^H is the

Hermitian of matrix \mathbf{G} and \mathbf{I} denotes the identity matrix. Orthogonality simplifies the implementation of a maximum-likelihood detector, because ILI can be canceled completely. In the case of ISI, however, orthogonality is getting lost and more complex detection algorithms must be applied such as maximum-likelihood sequence estimation.

In the case of molecular communication, the data symbols (amount of emitted molecules) are non-negative and real-valued rather than complex-valued. For OOK which is considered throughout this work, data bits are mapped onto data symbols $s_k \in \{0, N\}$ following the principle of (3). Hence, the classical Alamouti code has to be adapted to an Alamouti-type code that avoids the minus sign and the complex conjugate. As suggested in [24], the adaptation can be done by discarding the complex conjugate operation and replacing negative symbols by $\bar{s}_k := N - s_k$. As a result, the transmission matrix of the Alamouti-type code is given by

$$\mathbf{G} = \begin{bmatrix} s_k & s_{k+1} \\ N - s_{k+1} & s_k \end{bmatrix}. \quad (9)$$

B. Repetition MIMO Coding

A simple alternative to orthogonal Alamouti codes is offered by repetition MIMO [25]. In repetition MIMO the information is distributed over all transmit antennas, where each antenna transmit exactly the same data symbol at the same time. As a result, the transmission matrix for a 2×2 MIMO scenario is represented by

$$\mathbf{G} = \begin{bmatrix} s_k & s_k \end{bmatrix}. \quad (10)$$

A big advantage of repetition MIMO is that, even in the presence of ISI, single antenna detection algorithms can be applied. In addition, the ILI is constructive and contributes to the signal strength.

C. Equal-gain Combining

Before detection can be performed at Rx, the received signals of each receive antenna have to be combined/selected in a certain way. Following the equal-gain combining (EGC) algorithm, the signals of all receive antennas are equally weighted and combined:

$$y[k] = y_1[k] + y_2[k]. \quad (11)$$

Note that, for symmetrical scenarios, EGC is equivalent to MRC. In MRC, the combined signals are weighted by a factor that is proportional to the corresponding channel quality. For symmetrical scenarios, however, the channels at both receive antennas are the same. As a result, the channel description for the investigated scenario, can be further simplified. Considering that $h_{11}[\ell] = h_{22}[\ell]$ and $h_{12}[\ell] = h_{21}[\ell]$, (11) can be restated as

$$y[k] = \sum_{\ell=0}^L h[\ell] (x_1[k-\ell] + x_2[k-\ell]) + n[k], \quad (12)$$

where $h[\ell] \doteq h_{11}[\ell] + h_{12}[\ell]$ and $n[k] \doteq n_1[k] + n_2[k]$.

TABLE I
SIMULATION PARAMETERS USED FOR ANALYSIS. THE DEFAULT
PARAMETERS ARE IN BOLD FACE.

Parameter	Value
D [$\mu\text{m}^2/\text{s}$]	{50, 100 , 150, 200}
r [μm]	5
d [μm]	20
a [μm]	{ 11 , 13, 15, 17}
T_s [s]	0.6
L	3
N	{500, 1000 , 1500, 2000}
K	10^6
R	1000

V. DETECTION ALGORITHMS

For the bit error analysis throughout this paper, two different detection algorithms are considered and adopted from [26]. First of all, the low-complexity adaptive threshold detector (ATD) is applied, which works independent of explicit channel knowledge:

$$\hat{u}[k] = \begin{cases} 1 & \text{if } y[k] > y[k-1] \\ 0 & \text{if } y[k] \leq y[k-1]. \end{cases}$$

The second algorithm is maximum-likelihood sequence estimation (MLSE) based on the suboptimal squared Euclidean distance branch metric

$$\gamma(y[k] | [\hat{u}[k], \dots, \hat{u}[k-L]]) = \left(y[k] - \sum_{\ell=0}^L N \hat{h}[\ell] \hat{u}[k-\ell] \right)^2.$$

For a single antenna system $\hat{h}[\ell]$ is assumed to be equal to the channel coefficients from (5). For repetition coding with EGC $\hat{h}[\ell] = 2h[\ell]$, where $h[\ell]$ is defined as in (12).

In the case of Alamouti-type coding, the branch metric can be further adapted. Since the information of two bits is spread over two consecutive time slots, the branch metric can be evaluated jointly for both received numbers of molecules.

VI. NUMERICAL RESULTS

For simulative analysis, different parameters settings are considered. These are summarized in Table I, where K is the bit sequence length for one channel realization and R is the total number of channel realizations. It is assumed that after $(L+1)T_s = 2.4$ s the remaining ISI is negligible. In order to guarantee a fair comparison between the SISO and the 2×2 MIMO system by means of transmitting energy, the number of released molecules N in the case of the SISO scenario is set twice as large as for the MIMO case. Furthermore for the SISO scenario, there is just a single transmit and a single receive antenna present in the environment.

The effect of spatial diversity is examined by means of a BER analysis. We investigate how the BER is impacted by the number of molecules N , separation distance a , and diffusion coefficient D . This is done by varying one system parameter, while fixing the other ones to the bold-faced values in Table I.

Effect of Number of Emitted Molecules: In Fig. 3a, the effect of variation on the number of emitted molecules is shown. The

number of molecules is proportional to the signal strength. In fact, if N is increased, the variance lessens around the expected channel impulse response and more molecules hit the Rx sphere. Consequently, when N is increased, all detection algorithms achieve better performance when N is increased. ATD benefits from the ISI in the system [26]. The best BER performance, however, is achieved by MLSE. This is due to the fact that MLSE implies channel equalization, which counteracts ISI. Repetition MIMO with ATD slightly outperforms SISO transmission in a region with few molecules. However, the spatial diversity gain for ATD is not significant. For MLSE, the spatial diversity gain can be more clearly observed. The maximum BER improvement of repetition MIMO over the SISO case is by a factor of almost 10. A factor of almost 400 is achieved, when power normalization (the emitted number of molecules in the SISO case is twice as large as in the 2×2 MIMO case) is neglected. For the system considered here, Alamouti-type coding brings no BER improvement. The reason is that in case of repetition MIMO the ILI constructively contributes to the signal strength, whereas in Alamouti-type coding ILI is competitive and as a result more destructive.

Effect of Antenna Separation: Fig. 3b shows the effect of the antenna separation distance on the MIMO system performance. Thereby, all MIMO systems perform worse if the antenna separation distance is increased, because the spatial gain from ILI is decreased. For repetition MIMO with MLSE, a spatial diversity gain is still present for $a = 17 \mu\text{m}$.

Effect of Diffusion Coefficient: Fig 3c shows the effect of variation in the diffusion coefficient on the system performance. A larger diffusion coefficient leads to a more spiky channel impulse response. As a result, all detection algorithms under consideration achieve a smaller BER if the diffusion coefficient is increased. The spatial diversity gain from repetition MIMO with ATD increases with D . However, the spatial diversity gain is not significant. The gap between repetition MIMO with MLSE and the SISO MLSE case is constant by a factor of around 10 for the analyzed parameters. As in Fig. 3a-3b, Alamouti-type coding does not show any spatial diversity gain compared to a SISO system.

VII. CONCLUSION

In this paper, a diffusion-based molecular 2×2 MIMO communication system in a 3-D environment was presented. Channel coefficients were obtained from a trained ANN and incorporated into performance evaluations. Motivated from the potential of spatial diversity in classical wireless communication, different spatial diversity algorithms were introduced to the area of MC and their performances were analyzed. In detail, Alamouti-type coding and repetition MIMO coding were proposed at the transmitter side. At the receiver side, equal-gain combining that is equivalent to MRC in symmetrical scenarios, was presented as a receiver combining strategy. In addition, adaptive threshold detection and maximum-likelihood sequence estimation were adapted to the 2×2 MIMO scenario. The diversity gain was analyzed by numerical

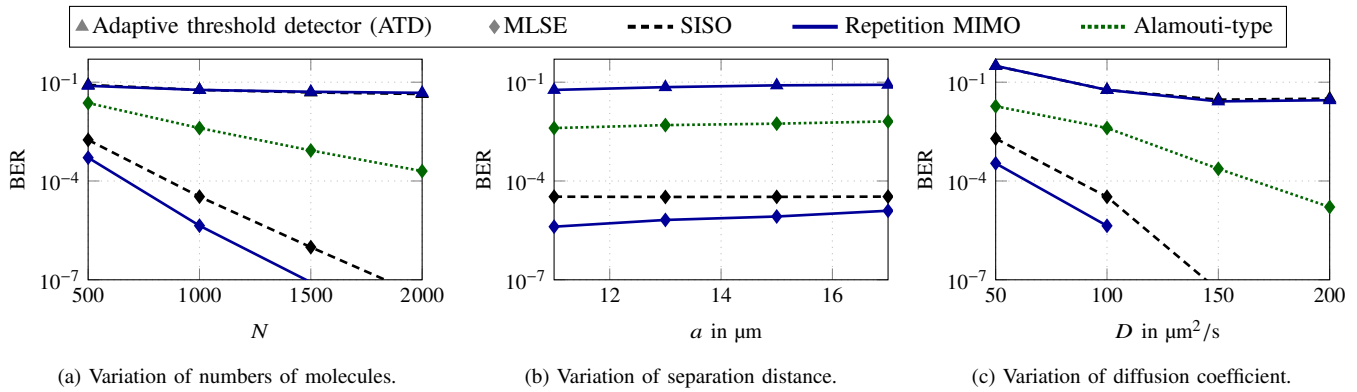


Fig. 3. Bit error rate performance as a function of the number of molecules (a), separation distance (b), and diffusion coefficient (c). If the corresponding parameter is not varying, it is fixed to $N = 1000$, $a = 11 \mu\text{m}$, and $D = 100 \mu\text{m}^2/\text{s}$.

simulations. We leave practical algorithms for unsymmetrical cases for our future work.

ACKNOWLEDGMENT

The work of H. B. Yilmaz and C.-B. was in part supported by the Basic Science Research Program (2017R1A1A1A05001439) through the NRF of Korea.

REFERENCES

- [1] N. Farsad, H. B. Yilmaz, A. Eckford, C.-B. Chae, and W. Guo, "A comprehensive survey of recent advancements in molecular communication," *IEEE Commun. Surveys Tuts.*, vol. 18, no. 3, pp. 1887–1919, 2016.
- [2] Y. Xia, P. Yang, Y. Sun, Y. Wu, B. Mayers, B. Gates, Y. Yin, F. Kim, and H. Yan, "One-dimensional nanostructures: synthesis, characterization, and applications," *Wiley Adv. Mater.*, vol. 15, no. 5, pp. 353–389, 2003.
- [3] W. Guo, T. Asyhari, N. Farsad, H. B. Yilmaz, B. Li, A. Eckford, and C.-B. Chae, "Molecular communications: channel model and physical layer techniques," *IEEE Wireless Commun. Mag.*, vol. 23, no. 4, pp. 120–127, 2016.
- [4] T. Nakano, A. W. Eckford, and T. Haraguchi, *Molecular communication*. Cambridge University Press, 2013.
- [5] M. Pierobon and I. F. Akyildiz, "A physical end-to-end model for molecular communication in nanonetworks," *IEEE J. Sel. Areas Commun.*, vol. 28, no. 4, pp. 602–611, May 2010.
- [6] A. Noel, K. C. Cheung, and R. Schober, "Optimal receiver design for diffusive molecular communication with flow and additive noise," *IEEE Trans. NanoBiosci.*, vol. 13, no. 3, pp. 350–362, 2014.
- [7] L.-S. Meng, P.-C. Yeh, K.-C. Chen, and I. F. Akyildiz, "MIMO communications based on molecular diffusion," in *Proc. IEEE Glob. Commun. Conf. (GLOBECOM)*, Dec. 2012, pp. 5380–5385.
- [8] B.-H. Koo, C. Lee, H. B. Yilmaz, N. Farsad, A. Eckford, and C.-B. Chae, "Molecular MIMO: From theory to prototype," *IEEE J. Sel. Areas Commun.*, vol. 34, no. 3, pp. 600–614, Mar. 2016.
- [9] Y. Lu, M. D. Higgins, A. Noel, M. S. Leeson, and Y. Chen, "The effect of two receivers on broadcast molecular communication systems," *IEEE Trans. NanoBiosci.*, vol. 15, no. 8, pp. 891–900, Dec. 2016.
- [10] C. Lee, B. Koo, N.-R. Kim, H. B. Yilmaz, N. Farsad, A. Eckford, and C.-B. Chae, "Molecular MIMO communication link," in *Proc. IEEE Int. Conf. on Comput. Commun. Workshops (INFOCOM WKSHPS)*, 2015, pp. 13–14.
- [11] K. Srinivas, A. W. Eckford, and R. S. Adve, "Molecular communication in fluid media: The additive inverse Gaussian noise channel," *IEEE Trans. Inf. Theory*, vol. 58, no. 7, pp. 4678–4692, 2012.
- [12] H. B. Yilmaz, A. C. Heren, T. Tugcu, and C.-B. Chae, "Three-dimensional channel characteristics for molecular communications with an absorbing receiver," *IEEE Commun. Lett.*, vol. 18, no. 6, pp. 929–932, Jun. 2014.
- [13] M. S. Kuran, H. B. Yilmaz, T. Tugcu, and I. F. Akyildiz, "Modulation techniques for communication via diffusion in nanonetworks," in *Proc. IEEE Int. Conf. on Commun. (ICC)*, 2011, pp. 1–5.
- [14] H. B. Yilmaz and C.-B. Chae, "Simulation study of molecular communication systems with an absorbing receiver: Modulation and ISI mitigation techniques," *Elsevier Simul. Model. Pract. Theory*, vol. 49, pp. 136–150, 2014.
- [15] N.-R. Kim and C.-B. Chae, "Novel modulation techniques using isomers as messenger molecules for nano communication networks via diffusion," *IEEE J. Sel. Areas Commun.*, vol. 31, no. 12, pp. 847–856, 2013.
- [16] M. J. Moore and T. Nakano, "Oscillation and synchronization of molecular machines by the diffusion of inhibitory molecules," *IEEE Trans. NanoTechnol.*, vol. 12, no. 4, pp. 601–608, Jul. 2013.
- [17] M. U. Mahfuz, D. Makrakis, and H. T. Mouftah, "On the characterization of binary concentration-encoded molecular communication in nanonetworks," *Elsevier Nano Commun. Netw.*, vol. 1, no. 4, pp. 289–300, 2010.
- [18] I. Llatser, A. Cabellos-Aparicio, M. Pierobon, and E. Alarcón, "Detection techniques for diffusion-based molecular communication," *IEEE J. Sel. Areas Commun.*, vol. 31, no. 12, pp. 726–734, Dec. 2013.
- [19] M. Damrath, S. Korte, and P. Hoehner, "Equivalent discrete-time channel modeling for molecular communication with emphasize on an absorbing receiver," *IEEE Trans. NanoBiosci.*, vol. 16, no. 1, pp. 60–68, Jan. 2017.
- [20] G. Genc, Y. E. Kara, H. B. Yilmaz, and T. Tugcu, "ISI-aware modeling and achievable rate analysis of the diffusion channel," *IEEE Commun. Lett.*, vol. 20, no. 9, pp. 1729–1732, 2016.
- [21] H. B. Yilmaz and C.-B. Chae, "Arrival modelling for molecular communication via diffusion," *IET Electron. Lett.*, vol. 50, no. 23, pp. 1667–1669, 2014.
- [22] C. Lee, H. B. Yilmaz, C.-B. Chae, N. Farsad, and A. Goldsmith, "Machine learning based channel modeling for molecular MIMO communications," *Proc. IEEE Int. Workshop on Sig. Proc. Advances in Wireless Comm. (SPAWC)*, also available at *arXiv:1704.00870*, Jul. 2017.
- [23] S. M. Alamouti, "A simple transmit diversity technique for wireless communications," *IEEE J. Sel. Areas Commun.*, vol. 16, no. 8, pp. 1451–1458, Oct. 1998.
- [24] M. K. Simon and V. A. Vilnrotter, "Alamouti-type space-time coding for free-space optical communication with direct detection," *IEEE Trans. Wireless Commun.*, vol. 4, no. 1, pp. 35–39, Jan. 2005.
- [25] S. G. Wilson, M. Brandt-Pearce, Q. Cao, and M. Baedke, "Optical repetition MIMO transmission with multipulse PPM," *IEEE J. Sel. Areas Commun.*, vol. 23, no. 9, pp. 1901–1910, Sep. 2005.
- [26] M. Damrath and P. A. Hoehner, "Low-complexity adaptive threshold detection for molecular communication," *IEEE Trans. NanoBiosci.*, vol. 15, no. 3, pp. 200–208, Apr. 2016.